ORIGINAL PAPER

www.pss-a.com

Solution-Processed, Insoluble Thin Films through In Situ Chemical Polymerization of Semiconducting Native Polythiophene

Jenny Lebert, Eva M. Kratzer, and Eva M. Herzig*

The use of multilayer, solution-processed organic thin film devices can benefit strongly from the controlled deposition of insoluble thin films. Here, a solution-based in situ polymerization technique for semiconducting polythiophene thin films based on nonchlorinated solvents forming a range of large-scale structured or homogeneous, insoluble thin films is systematically developed. The high-quality nature of the resulting polythiophene thin films is demonstrated by successfully implementing the films in the active layer of bilayer heterojunction solar cells. It is possible to transfer this protocol to large-scale processing without additional changes to the material system.

1. Introduction

Future organic electronic devices will consist of thin films with strongly tailored properties that need to be producible on a large scale and insensitive to further processing steps. Already today, innovative technologies such as organic light-emitting diodes (OLEDS), organic field-effect transistors (OFETS), and organic solar cells are benefitting from adaptable nanostructures and simple preparation routes.[1–7] The solution processability has already facilitated some upscaling of the fabrication, making a cost-efficient roll-to-roll production of devices in varied size regimes feasible.[8,9] Much of the material development is therefore focused on soluble materials. Insoluble materials

like unsubstituted conjugated polymers, such as native polythiophene (PT), which show very poor solubility are much less investigated due to the currently difficult preparation routes. However, the monomeric components often are still soluble. Nevertheless, such polymers are worth looking into, as they are known to exhibit a higher stability than their substituted derivatives. Due to their closer packing structure, the permeation of small degrading molecules such as, for example, oxygen is strongly reduced.[10,11] Furthermore, their insolubility can be further exploited during processing, e.g., when adding subsequent layers. However, producing homogeneous thin films out of unsubstituted conjugated polymers, particularly from solution, is challenging. An easily and cheaply available material system is thiophene. So far, organic solar cells have already been manufactured and investigated with native PT deposited by oxidative chemical vapor deposition (oCVD), solution processing of a soluble derivative followed by a high-temperature posttreatment to cut off the side chains, evaporation, or by electropolymerization.[11–14] While all of these procedures provide thin films of PT, they all suffer from either high material costs, restrictions in choice of substrate, or high energy consumption. We present here an all-solution-based method to produce insoluble PT thin films and demonstrate the scalability of the method using in situ polymerization. Starting with a metastable reaction mixture of monomer bithiophene (BT) and oxidizing agent phosphomolybdic acid hydrate (PMA), it is possible to trigger the polymerization reaction upon evaporation of the solvent and consequently increased concentrations of the two reactants.[15]

With this method it is possible to fabricate conducting, doped PT films. We use this as a starting point to further develop chemical protocols to solution process homogeneous, insoluble semiconducting PT films that are polymerized after deposition of the solution. We successfully turn these PT films into organic solar cells that are easily as efficient as prepared with vacuum deposition methods. Furthermore, we demonstrate the adaptability of the presented synthesis to a thin film fabrication by different types of solution deposition methods. We have shown elsewhere that the intrinsic reaction mechanism of such oxidative in situ polymerization of PT can be exploited for improving the intermolecular electronic interactions between the PT polymer chains by altering their crystal structure.[16] We believe that integrating the material synthesis into the deposition process will eventually allow to apply a wide range of control

Dr. J. Lebert
Herzig Group
Munich School of Engineering
Technische Universität München
Lichtenbergstraße 4a, 85748 Garching, Germany

E. M. Kratzer
Lehrstuhl für Chemische Verfahrenstechnik, Ingenieurwissenschaften
Universität Bayreuth
Universitätsstraße 30, 95447 Bayreuth, Germany

Prof. E. M. Herzig
Dynamik und Strukturbildung – Herzig Group, Experimentalphysik
Universität Bayreuth
Universitätsstraße 30, 95447 Bayreuth, Germany
E-mail: eva.herzig@uni-bayreuth.de

mechanisms to tailor the material properties on the nanoscale for a large variety of materials.

2. Results and Discussion

In organic electronic devices, film quality of the single functional layers is of utmost importance. The fabrication routine of choice needs to provide reproducible, homogeneous polymer films of adjustable thickness to ensure an optimized interaction of the single layers in the device stack. In an initial approach, we fabricated PT layers by adaption of the synthesis presented by Bravo-Grimaldo et al.[15] For this purpose, we prepared meta-stable reaction mixtures of BT and PMA in acetonitrile according to the original instruction. Upon spin coating this solution, the polymerization reaction yields insoluble PT films in their doped state (Figure S1, Supporting Information). Subsequently, we rinsed the films in ethanol and thermally annealed them. Rinsing in ethanol is known to have two effects, namely, the removal of undesired reaction by-products from the films and additionally the dedoping of the polymer to its neutral, semi-conducting state.[12,16] However, these semiconducting films (Figure S1, Supporting Information) show large inhomogeneities on the micrometer scale as shown by means of optical microscopy (**Figure 1**a,b). At low magnification (Figure 1a), the microscopy images reveal that the used in situ polymerization generates polymer films without the formation of any large grains or aggregates. At larger magnification, however, the films exhibit a large-scale pattern due to cracks in the film surface (Figure 1b). These cracks are detrimental for the solar cell performance, and bilayer heterojunction solar cell devices created from such films in combination with PCBM as electron acceptor material showed simply a resistive behavior. This is naturally explained by the large cracked thin film structure leading to current leaks between the two electrodes. While such a regular 10 µm structure might be beneficial for some applications, solar cells require a homogeneous surface structure on this and lower length scales.

To improve the film quality, we systematically examined alternative solution-based approaches for the in situ synthesis of semiconducting PT. We replaced the oxidizing agent PMA with iron(III) p-toluenesulfonate (FeTos). FeTos has been introduced by Bayer for the in situ polymerization of poly(3,4-ethylenedioxythiophene) (PEDOT) from solution.[17] Since then, it has been employed as oxidant for the synthesis of high-quality PEDOT films with different fabrication techniques and for various electronic applications.[18–21] Moreover, Kolodziejczyk et al. have used FeTos in the vapor-phase poly-merization of PT.[22,23] For a polymerization of PT from solu-tion, it has not been used by other groups so far. Starting from the broad knowledge of in situ PEDOT polymerization pro-cesses, we identified alcoholic solvents as ideal solvents for the metastable reaction mixtures. To find optimal reaction conditions, we prepared solutions in ethanol, propanol, and butanol, respectively. Other than in the PEDOT fabrication, however, spin coating the solution at room temperature fol-lowed by a subsequent heating step does not result in homoge-neous polymer films, although the polymerization reaction does take place. Therefore, we used a spin coater with heated sub-strate plate to ensure a steady heating of substrate and solution during the deposition and spinning process. The required tem-perature depends strongly on the boiling temperature of the respective used solvent, increasing from about 60 °C for ethanol to 100 °C for butanol. In our studies we identify that the fabri-cation from propanol at 90 °C results in the most homogeneous films. Also, for this oxidizing agent we can obtain both conduct-ing and semiconducting thin films.[16] Here, we demonstrate the successful application of the ethanol-rinsed semiconducting films for use in solar cells.

Therefore, the macroscale quality of the PT thin films after ethanol-rinsing and thermal annealing is presented again by optical microscopy (Figure 1c,d). The optical micrographs reveal
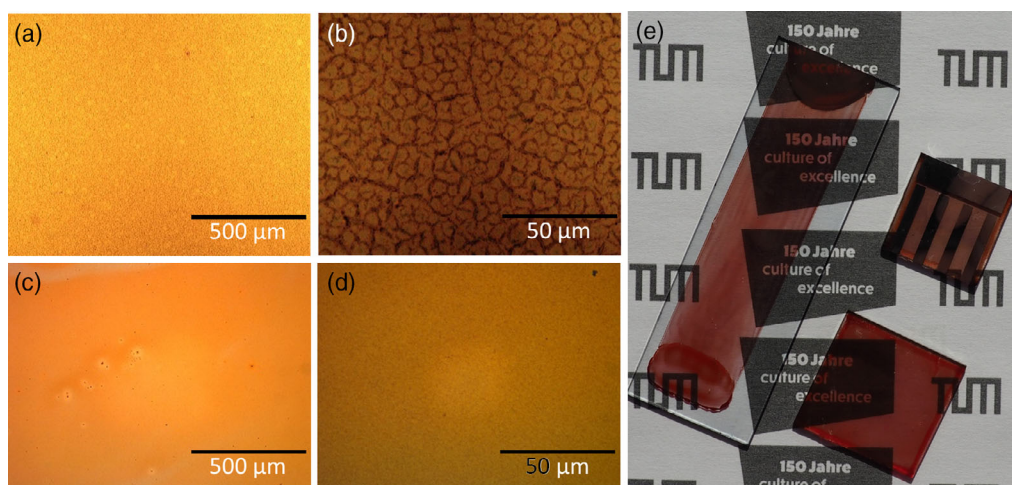

Figure 1. Optical micrographs of semiconducting PT thin films after thermal annealing. a,b) Film morphology derived from synthesis with PMA as oxidizing agent featuring major cracks throughout the whole visible area. c,d) Significant improvement in film homogeneity and quality by application of FeTos as oxidant instead. e) Photograph of polythiophene samples prepared with the presented in situ polymerization of semiconducting PT thin films: slot-die printed sample (left; 7.5 × 2.5 cm^2), spin coated sample (bottom right; 2.5 × 2.5 cm^2), and lab-scale solar cell (top right; 2.0 × 2.0 cm^2).
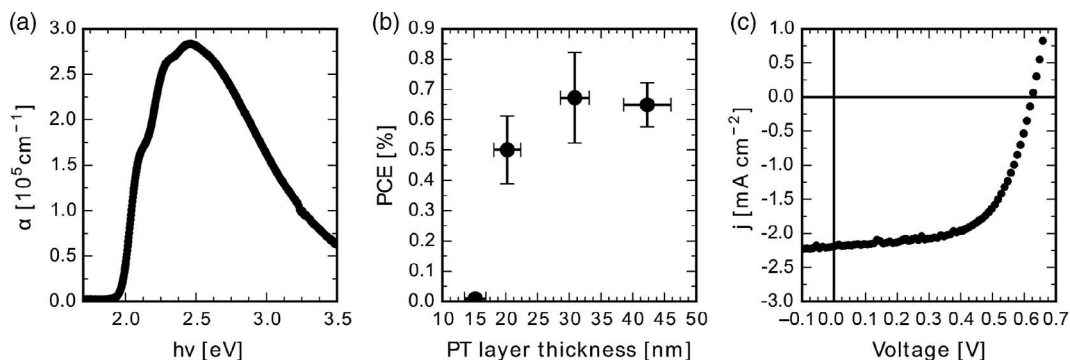
Figure 2. Optical properties and solar cell performance of PT thin films synthesized with FeTos as oxidizing agent. a) Absorption coefficient α as a function of photon energy of ethanol rinsed thin film. b) Power conversion efficiency of bilayer heterojunction PT:PCBM devices in dependence of PT layer thickness, error bars correspond to standard deviations of given mean values. c) I–V characteristic of single champion cell with PCE of 0.8%.

the high homogeneity of the obtained films. We do not observe any surface cracks that are obtained when the synthesis is performed with PMA.

These homogeneous films are further characterized by determining their absorption coefficient $\alpha(\lambda)$ by means of absorption spectroscopy (**Figure 2**a).

The PT shows an absorption over a broad energy range with vibronic shoulders in the low-energy regime and a featureless absorbance at energies beyond the absorbance maximum. With a maximum of 2.8×10^5 cm^{-1} at 504 nm, the absorption coefficient is similar to that for PT synthesized, for example, by oCVD.[24] The peak at this wavelength is in accordance with that of PT values showing that the polymerization was successful. Small, weakly polymerized components absorb at energies above 2.75 eV (i.e., below 450 nm)[25] where no dominant contributions are present after the rinsing procedure (Figure 2a). The observed $\alpha(\lambda)$ is more than 3 times higher than that of crystalline P3HT films due to the missing volume of the optically inactive side chains.[26] By help of the Tauc equation, we determine the optical bandgap of our semiconducting PT to be $E_g = (1.91 \pm 0.02)$ eV.[27,28] Therefore, it is only slightly larger than that of P3HT which is reported to be between 1.85 and 1.9 eV.[29,30]

To further demonstrate the high quality of the film from our new improved process, we implement the PT films in the active layer of bilayer heterojunction solar cells with an active layer stack of PCBM on top of PT. For device optimization, we vary the PT layer thickness by variation of the concentrations of the two components in the reaction mixture. The resulting solar cell parameters for the cells with PT layer thicknesses ranging from 15 to 42 nm are summarized in **Table 1**. Upon increasing the

PT thickness, the performance of the solar cells is changing constantly, with a change in short-circuit current density (J_{SC}), open-circuit voltage (V_{OC}), fill factor (FF), and power conversion efficiency (PCE), respectively. Clearly, the thickness has an impact on several of the involved processes. Beyond a critical film thickness between 15 and 20 nm, however, the J_{SC} reaches high values for the examined material system.[31] Therefore, while most devices are not functioning for the thinnest tested layer of about 15 nm thickness, the performance is comparable and higher for thicknesses between 20 and 45 nm in comparison to PT solar cells made with oCVD.[12] Our champion cell, whose I–V characteristics are shown in Figure 2c, even reached an efficiency of 0.8%. Therefore, our solution-based in situ synthesis of semiconducting PT films enables the production of devices that exhibit the same range of efficiencies as the ones prepared from oCVD, evaporation, or by using a high-temperature thermocleavage step.[11–13] Such solution-processed layers would also be possible to be applied as thin protecting layers for subsequent solution deposition of different materials in semiconducting devices.

Finally, we want to address the potentials of adapting the synthesis to different solution deposition techniques. A major advantage of a solution-based thin film deposition is the flexibility with regard to used fabrication technique and the potential upscaling to larger substrates by, for example, roll-to-roll printing.[8] To investigate whether the synthesis developed here is transferable from spin coating to other solution deposition processes, the metastable reaction mixture is deposited to larger substrates by means of slot-die coating. In Figure 1e, we demonstrate the transferability of the in situ polymerization process out of solution from spin coating to printing. The typical semitransparency and color of the rinsed and temperature annealed film shows the successful polymerization process for both deposition techniques. The BT monomers or short chains would have a yellow color. For this purpose, a custom-made lab-scale printing setup is used, which enables a constant heating of the substrate plate.[32] For in situ polymerization during printing, the synthetic routine previously optimized for spin coating is maintained in terms of solution composition, substrate temperature, and posttreatment routine. The photograph shows a large printed film in comparison to the spin coated PT film on glass as well as a lab-scale PT:PCBM solar cell. All presented sample types are

Table 1. Performance parameters of PT:PCBM bilayer heterojunction solar cells with varied PT layer thickness. Errors are standard deviations to given mean values of four solar cells each.

PT thick-ness [nm]	J_{SC} [mA cm^{-2}]	V_{OC} [V]	FF [%]	PCE [%]
15 ± 2	0.1 ± 0.1	0.38 ± 0.05	25 ± 1	0.01 ± 0.01
20 ± 3	1.7 ± 0.3	0.53 ± 0.03	53 ± 1	0.5 ± 0.2
31 ± 3	1.9 ± 0.3	0.60 ± 0.05	58 ± 3	0.7 ± 0.2
42 ± 4	1.7 ± 0.2	0.63 ± 0.01	60 ± 1	0.6 ± 0.1

fabricated from the polymerization technique developed here. Figure 1e shows the same absorption behavior of the films (semitransparency and color) for both fabrication routes. Therefore, we conclude that the established synthesis enables a film fabrication by different solution deposition techniques and is conveniently transferable to larger scale processes.

3. Conclusions

In conclusion, we have presented the successful development of a solution-based in situ polymerization of semiconducting PT for application in bilayer organic solar cells. By optimizing the reaction agent, solvent and temperature, we identify a solid protocol for the fabrication of PT thin films synthesized in situ during the film formation from a metastable reaction mixture. We demonstrate that the quality of the resulting films strongly depends on the used oxidizing agent. By appropriately adapting the synthesis parameters, we are able to fabricate high-quality PT films which result in functioning active layers for bilayer PT solar cells (<1%) with equivalent efficiencies as obtained by more complex methods. Finally, we demonstrate the flexibility of this solution-based in situ polymerization by transferring it to a slot-die coating process with large-scale production capabilities without further changes to the preparation routine.

4. Experimental Section

In Situ Polymerization with PMA: Prior to the synthesis, the used glass substrates were cleaned and covered with a layer of polystyrene sulfonate (Polymer Standards Service GmbH Mainz) spin coated from 1-chlorobenzene (synthesis grade; Roth). This adhesive layer was necessary to facilitate the adhesion between subsequently synthesized PT film and substrate. From our experience, most polymers such as polypropylene and polystyrene sulfonate and also PEDOT:PSS fulfilled that purpose. The PT films were prepared from metastable solutions of $0.10\,mol\,L^{-1}$ of monomer 2,2′-BT (Alfa Aesar) and $0.12\,mol\,L^{-1}$ of oxidizing agent PMA (Sigma-Aldrich) in acetonitrile (HPLC grade; Sigma-Aldrich). The solution was spin coated onto the substrate at 2000 rpm for 30 s at ambient temperature. Afterward, the films were dried for 30 min, rinsed in ethanol for another 30 min, and finally thermally annealed at 200 °C for 10 min at ambient atmosphere. All chemicals were used as purchased without further purification.

In Situ Polymerization with FeTos: The films were prepared on pretreated substrates as described earlier. Metastable solutions were prepared with $0.10\,mol\,L^{-1}$ of BT and $0.20\,mol\,L^{-1}$ of oxidizing agent FeTos (Sigma-Aldrich) in 1-propanol (synthesis grade; Roth). For in situ polymerization, the solution was spin coated at 2000 rpm for 60 s at 90 °C. If the slot-die printer was used, the print head-to-substrate distance was set to 0.3 mm, the solution was fed to the print head at $0.25\,mL\,min^{-1}$, the substrate moved below the print head at a velocity f $20\,mm\,s^{-1}$, and the substrate temperature was also set to 90 °C Details on the printer setup were thoroughly discussed in the publication by Pröller et al.[32] Finally, all films were rinsed in ethanol for 30 min and annealed at 200 °C for 10 min in ambient atmosphere. All chemicals were used as purchased without further purification.

Solar Cell Fabrication: The solar cells presented here were prepared as a layer stack of indium tin oxide (ITO)/PEDOT:PSS/PT/PCBM/aluminum. ITO-covered glass substrates ($2.0 \times 2.0\,cm^2$; Solems) were patterned manually by etching a 0.5 cm wide stripe of the ITO away with hydrochloric acid and zinc powder. Afterward, the substrates were cleaned and covered with a layer of PEDOT:PSS deposited from an aqueous dispersion (Al 4083; Ossila) by spin coating at 3000 rpm for 60 s followed by a thermal

annealing step at 150 °C for 10 min. Subsequently, a layer of PT was deposited, as described earlier, to serve as electron donor material. The layer thickness variation from 15 up to 42 nm was achieved by using precursor solutions with overall reactant concentrations of $0.06–0.15\,mol\,L^{-1}$ upon keeping the molar ratio between BT and FeTos at 1:2.

The electron acceptor PCBM (1-Material) was spin coated on top from a solution of $13.5\,mg\,mL^{-1}$ in chlorobenzene (≥99.5%; Roth) at 1000 rpm for 60 s. One hundred nanometer thick aluminum (99.99%; ChemPUR) electrodes were thermally evaporated at pressures below 10^{-5} mbar on top of the stack as last layer. Finally, the whole device was thermally annealed at 100 °C for 10 min in an inert atmosphere. All chemicals were used as purchased without further purification.

Film Characterization: To investigate the polymer film surface, the samples were investigated with a Leica DM2700 optical microscope combined with a charged coupled device (CCD) camera. The thin film absorbance $A(\lambda)$ was determined with a Lambda 650S spectrometer from PerkinElmer. The absorption coefficient $\alpha(\lambda)$ was determined according to $\alpha(\lambda) = A(\lambda)[(d[\log]10(e))]^{-1}$, with film thickness d. All film thicknesses used in the presented results were measured by profilometry using a Dektak XT from Bruker Nano Surfaces Division with a diamond tip of 2 μm radius. For device characterization, the solar cells were irradiated with a calibrated air mass 1.5 global solar spectrum (AM1.5; $100\,mW\,cm^{-2}$). The illuminated pixel size of $0.1\,cm^2$ was controlled by covering the device with an aluminum mask. The respective I–V characteristics were measured by connecting the solar cells to a Keithley 2400 source meter and detecting the current upon a voltage sweep from −1 to 1 V. To obtain the current density, the current was normalized by the active solar cell area.

Conflict of Interest

The authors declare no conflict of interest.

[1] J. H. Noh, S. H. Im, J. H. Heo, T. N. Mandal, S. I. Seok, *Nano lett.* **2013**, *13*, 1764.

[2] J. A. Rogers, T. Someya, Y. Huang, *Science* **2010**, *327*, 1603.

[3] S. R. Forrest, *Nature* **2004**, *428*, 911.

[4] S.-M. Lee, J. H. Kwon, S. Kwon, K. C. Choi, *IEEE Trans. Electron Dev.* **2017**, *64*, 1922.

[5] B. C. Thompson, J. M. J. Fréchet, *Angew. Chem. Int.* **2008**, *47*, 58.

[6] L. Antolini, G. Horowitz, F. Kouki, F. Garnier, *Adv. Mater.* **1998**, *10*, 382.

[7] M. Kaltenbrunner, M. S. White, E. D. Głowacki, T. Sekitani, T. Someya, N. S. Sariciftci, S. Bauer, *Nat. Commun.* **2012**, *3*, 770.

[8] R. R. Søndergaard, M. Hösel, F. C. Krebs, *J. Polym. Sci. B Polym. Phys.* **2013**, *51*, 16.

[9] A. C. Arias, J. D. MacKenzie, I. McCulloch, J. Rivnay, A. Salleo, *Chem. Rev.* **2010**, *110*, 3.

[10] F. C. Krebs, H. Spanggaard, *Chem. Mater.* **2005**, *17*, 5235.

[11] S. A. Gevorgyan, F. C. Krebs, *Chem. Mater.* **2008**, *20*, 4386.

[12] D. C. Borrelli, M. C. Barr, V. Bulović, K. K. Gleason, *Sol. Energy Mater. Sol. Cells* **2012**, *99*, 190.

[13] P. Kovacik, H. E. Assender, A. A. R. Watt, *Sol. Energy Mater. Sol. Cells* **2013**, *117*, 22.

[14] R. Valaski, C. D. Canestraro, L. Micaroni, R. M. Q. Mello, L. S. Roman, *Sol. Energy Mater. Sol. Cells* **2007**, *91*, 684.

[15] E. Bravo-Grimaldo, S. Hachey, C. G. Cameron, M. S. Freund, *Macromolecules* **2007**, *40*, 7166.

[16] J. Lebert, E. M. Kratzer, A. Bourdick, M. Coric, S. Gekle, E. M. Herzig, *ACS Omega* **2018**, *3*, 6388.

[17] F. Jonas, G. Heywang, W. Schmidtberg, J. Heinze, M. Dietrich, Canada Patent CA1337950C, **1988**.

[18] B. Winther-Jensen, M. Forsyth, K. West, J. W. Andreasen, P. Bayley, S. Pas, D. R. MacFarlane, *Polymer* **2008**, *49*, 481.

[19] O. Bubnova, Z. U. Khan, H. Wang, S. Braun, D. R. Evans, M. Fabretto, P. Hojati-Talemi, D. Dagnelund, J.-B. Arlin, Y. H. Geerts, S. Desbief, D. W. Breiby, J. W. Andreasen, R. Lazzaroni, W. M. Chen, I. Zozoulenko, M. Fahlman, P. J. Murphy, M. Berggren, X. Crispin, *Nat. Mater.* **2014**, *13*, 190.

[20] Z. U. Khan, O. Bubnova, M. J. Jafari, R. Brooke, X. Liu, R. Gabrielsson, T. Ederth, D. R. Evans, J. W. Andreasen, M. Fahlman, X. Crispin, *J. Mater. Chem. C* **2015**, *3*, 10616.

[21] J. P. Lock, S. G. Im, K. K. Gleason, *Macromolecules* **2006**, *39*, 5326.

[22] B. Kolodziejczyk, D. Mayevsky, B. Winther-Jensen, *RSC Adv.* **2013**, *3*, 4568.

[23] B. Kolodziejczyk, O. Winther-Jensen, R. Kerr, P. Firbas, B. Winther-Jensen, *React. Funct. Polym.* **2015**, *86*, 60.

[24] D. C. Borrelli, S. Lee, K. K. Gleason, *J. Mater. Chem. C* **2014**, *2*, 7223.

[25] S. Nejati, K. K. S. Lau, *Langmuir* **2011**, *27*, 15223.

[26] U. Zhokhavets, T. Erb, G. Gobsch, M. Al-Ibrahim, O. Ambacher, *Chem. Phys. Lett.* **2006**, *418*, 347.

[27] J. Tauc, R. Grigorovici, A. Vancu, *Phys. Stat. Sol. B* **1966**, *15*, 627.

[28] N. Ghobadi, *Int. Nano Lett.* **2013**, *3*, 465.

[29] M. Wright, A. Uddin, *Sol. Energy Mater. Sol. Cells* **2012**, *107*, 87.

[30] R. Kroon, M. Lenes, J. C. Hummelen, P. W. M. Blom, B. de Boer, *Polym. Rev.* **2008**, *48*, 531.

[31] G. Li, R. Zhu, Y. Yang, *Nat. Photonics* **2012**, *6*, 153.

[32] S. Pröller, D. Moseguí González, C. Zhu, E. Schaible, C. Wang, P. Müller-Buschbaum, A. Hexemer, E. M. Herzig, *Rev. Sci. Inst.* **2017**, *88*, 66101.